Accepted Manuscript

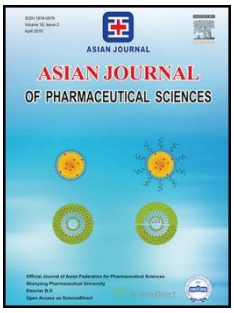

Title: *In silico* product design of pharmaceuticals

Author: Johan Boetker, Dhara Raijada, Johanna Aho, Milad Khorasani, Søren Vinter Søgaard, Lærke Arnfast, Adam Bohr, Magnus Edinger, Jorrit Water, Jukka Rantanen

PII: S1818-0876(16)30009-5
DOI: http://dx.doi.org/doi: 10.1016/j.ajps.2016.02.010
Reference: AJPS 362

To appear in: *Asian Journal of Pharmaceutical Sciences*

Received date: 8-10-2015
Accepted date: 14-2-2016

Please cite this article as: Johan Boetker, Dhara Raijada, Johanna Aho, Milad Khorasani, Søren Vinter Søgaard, Lærke Arnfast, Adam Bohr, Magnus Edinger, Jorrit Water, Jukka Rantanen, *In silico* product design of pharmaceuticals, *Asian Journal of Pharmaceutical Sciences* (2016), http://dx.doi.org/doi: 10.1016/j.ajps.2016.02.010.

In silico product design of pharmaceuticals

Johan Boetker, Dhara Raijada, Johanna Aho, Milad Khorasani, Søren Vinter Søgaard, Lærke Arnfast, Adam Bohr, Magnus Edinger, Jorrit Water, Jukka Rantanen*

Department of Pharmacy, Faculty of Health and Medical Sciences, University of Copenhagen, Denmark

Corresponding author:

Jukka Rantanen
Professor, Ph.D.
University of Copenhagen
Faculty of Health and Medical Sciences
Department of Pharmacy
Universitetsparken 2
2100 Copenhagen
Denmark
Tel: +45 35 33 65 85
Fax: +45 35 33 60 30
Email: jukka.rantanen@sund.ku.dk

Abstract

The increasing demand for personalized medicine necessitates the production of easily customizable dosage forms. As the number of possible dosage forms may scale towards infinity, their uniqueness require a versatile production platform and numerical simulation in order to be manufactured efficiently. A mathematical description of these systems is the only feasible approach to manage such diverse properties of different products. However, experimental verification is still essential for evaluation of processability and related concomitant phenomena, such as possible solid state changes that may occur during production and storage.

Keywords

Personalized medicine, simulation, rheology, imaging, continuous manufacturing, extrusion

1. Introduction

Future manufacturing lines for pharmaceutical production will increasingly be based on continuously operating lines that enable flexible dosing of pharmaceuticals for personalized needs.[1] These tailor-made medicinal products may rely on recent innovations within genomics and diagnostics, which can be used as an input for defining patient's individual dosing regimes. Conceivably also the patient's dose may be adjusted according to input from e.g. telemedicine devices that have online data monitoring and can gather important biological and clinical parameters such as blood plasma concentrations of the drug compound measured.[2, 3] Based on these possibilities, there is a need for more fundamental research enabling a manufacturing-on-demand based health-care system[4] and drug product development based on therapy-driven target drug delivery profiles.[5]

One approach for flexible dosing is hot melt extrusion (HME) based production that enables manufacturing of innovative product shapes that can be easily divided into the required dose.[6, 7] The manufacturing of such dosage forms in a personalized medicine scenario requires continuous monitoring of the product in order to assure that it complies with the desired drug loading and product consistency.[1] HME provides the possibility to process medicines into desired size and shape using various die geometries. Circular dies can be used for producing rods that can subsequently be pelletized or spheronized, or flat dies may be used for the production of films. Furthermore, downstream injection molding provides an even broader array of possible sizes and shapes of the final product.[8] Finally, the emerging capabilities of 3D printing production platforms provides infinite possibilities for manipulation of the final product size and shape (limited by resolution) and could become the leading production platform for personalized medicine.[9] The recent FDA approval of SPRITAM, a 3D printed orally dissolving tablet, further emphasizes that 3D printing is a viable method for production of innovative drug formulations.[10]

Many pharmaceutical processes, including HME, require a powder feed. Powder feeding into an extruder may necessitate a flow in a restricted geometry similar to powder flow in a hopper. Numerous investigations on powder flow in hoppers and silos have been performed during the last century and many of these investigations has been based on Janssen's work dating back to 1895.[11] More recent efforts to solve the pressures persisting within these loaded silo and hopper structures by finite element modelling have also been pursued.[12-16] In addition, HME processing typically involves production of a molten polymer-active compound mixture, and once extruded, the solid state composition of the mixture can have an impact on the product properties, such as mechanical strength and dissolution rate. One of the most critical quality attributes of these products is achieving a stable solid form composition, and possible changes to the solid form during processing can have a significant impact on the product quality. As for example shown by Young *et al.*, hot-melt extruded products can

recrystallize from the amorphous state.[17] It is therefore important to design the processing conditions such that an optimal product can be produced.

In any process involving polymer melts, including HME, understanding the rheology of the polymeric excipients is of crucial importance. Moreover, the addition of active pharmaceutical ingredients (APIs) can significantly affect the flow properties of polymer melts: many small molecule APIs that are soluble in the polymeric excipients used in HME, can act as plasticizers, and thereby decrease the viscosity of the melt compared to the pure polymer.[18-21] At concentrations beyond the solubility limit, the API is suspended as solid material, which may increase the viscosity of the melt.[21] Melt flow processes of polymers and their mixtures involve complex rheology due to their non-Newtonian and viscoelastic behavior. Additionally, flow behavior of highly filled dispersions increases the difficulty in prediction of the extrusion process outcome and necessitates the understanding of the fundamental rheological properties. Simulation of the hot melt extrusion process can reduce costs and development time compared to trial-and-error approaches, making it an efficient tool in the product and process design phase, and when scaling up the process for mass production. For an accurate and reliable HME simulation, material parameters such as melt density, heat transfer properties, and viscosity as a function of temperature and shear rate must be characterized.[22] ENREF 21

It is often beneficial to obtain an insight into these factors by a computational approach. Therefore, in addition to the experimental part, we report a computational approach (*in silico* product design). The primary aim of the computations was to evaluate the mechanical properties and dissolution rate of the extrudates and, the secondary aim was to evaluate the stresses within a hopper representing the powder feeding system for an extruder.

2. Material and methods

The finite element method (FEM) was utilized for the computational approach by numerical analysis. COMSOL Multiphysics v. 4.4. (Stockholm, Sweden) was used to build the geometry of the extrudate and powder hopper as well as to construct the mesh and to solve the partial differential equation systems.

For the experimental approach, a model formulation consisting of nitrofurantoin monohydrate and PEO was used. The extrusion was performed on a 5 ml lab scale extruder (Xplore micro compounder, Geleen, The Netherlands) equipped with two co-rotating screws, three individually controlled heating zones, and a recycling channel that enables recirculation of the melt within the

barrel. The API-polymer mixture was fed into the hopper manually. After the desired recirculation time, the melt was extruded through a circular die (Ø =15 mm), and the extrudates were cooled at room temperature.

XRPD measurements on the extrudates were performed using an X'Pert PRO θ/θ X-ray diffractometer (PANalytical, Almelo, Netherlands). The diffractograms were obtained in Bragg−Brentano reflection mode utilizing a PIXel detector (PANalytical). The operating voltage and current were 45 kV and 40 mA, respectively. A continuous scan over 2θ was performed in the range from 4-40° with a step time of 96.4 s/point and a point resolution of 0.026°.

NIR-chemical (NIR-CI) images of the extrudates were obtained with a spectrometer (Headwall Photonics model 1002A-00371, Fitchburg, MA, USA). This NIR chemical imaging camera is a prototype kindly provided by FOSS (FOSS A/S, Hilleroed, Denmark). NIR-chemical images of extrudates were recorded in the wavelength range of 1100–1700 nm. The spectrometer was adapted to a line mapping configuration with a line consisting of 320 pixels. Spectra were recorded in diffuse reflectance mode with a resolution of 50 x 312 µm/pixel.

NIR-CI data processing was performed using MATLAB 7.1 (The Math-Works, Natick, MA) software and in-house routines under the name of HYPER-Tools (freely available on demand) together with PLS Toolbox (Eigenvector Research Inc., Wenatchee, USA). Since the raw data from NIR-CI measurement consists of information both from the sample and from the instrument, background correction is necessary. The high reflectance standard Spectralon TM (Labsphere, Inc., North Sutton, New Hampshire, USA) was used as a background reference. Areas containing non-sample information were eliminated by masking. Standard Normal Variate transformation, Savitzky-Golay smoothing with window size of 13 and polynomial order of 2, together with mean-centering were applied as pre-processing methods.

Measurement of flow properties of polyethylene oxide (PEO) was used as an example of a widely used polymeric excipient in pharmaceutical applications. PEO melt (viscosity average molecular weight M_v= 100.000 g/mol) was characterized in steady state rotational shear (SS) and small angle oscillatory shear (SAOS) at three different temperatures using an AR-G2 stress-controlled rotational rheometer (TA Instruments, New Castle, DE, USA) with a 25 mm parallel plate geometry. Different viscosity models can be used to capture the flow behavior of such polymers to enable the flow predictions for process simulations. The Carreau-Yasuda viscosity model (Eq.1)

$$\eta(\dot{\gamma}) = \eta_0 \left[1 + (\lambda\dot{\gamma})^a\right]^{\frac{n-1}{a}} \quad (1)$$

was fitted to the superimposed SAOS and SS data at each temperature. The model has four fitting parameters: η_0 = zero-shear viscosity, n = power-law coefficient, λ = characteristic relaxation time, and the parameter a, which determines the sharpness of the shift from the zero-shear to power-law region. The fitting was performed using the non-linear fitting with least-squares method in GraphPad Prism 6 software (La Jolla, CA, USA), with the parameter constrains $\eta_0, \quad \lambda, \quad a < 0,$ and $0 < n < 1$.

3. Results and Discussion

3.1. In silico product design

3.1.1. Simulation of process equipment geometry

The computational approach can be utilized to design innovative engineering solutions and processing equipment. One of the remaining challenges within engineering of solid dosage forms is the calculation of stresses within a hopper filled with powder, such as the feeding system for an extruder (Fig. 1). Calculation of stress can be used to evaluate the powder flowability and flow patterns, i.e. to evaluate whether the system exhibits mass flow, funnel flow, or no flow at all. It should also be mentioned that simulation of the heat, mixing pressure, and material transfer in various screw elements within an extruder has previously been described in the literature.[23-25]

The stresses within the hopper can be calculated using measured or estimated values for Young's modulus (e.g. 200 MPa), density (e.g. 366 kg/m^3), wall static frictional coefficient (e.g. 0.73), and Poisson's ratio (e.g. 0.3) (Fig. 2a and b). Based on these calculations, the optimal design of the processing equipment that accommodates acceptable stresses within the powder prior to (Fig. 2a) and during extrusion can be identified (Fig. 2b) in order to avoid flow problems, such as segregation, stagnant zones and arching.[26]

3.1.2. Simulation of the mechanical properties of the drug product

The mechanical properties of extrudates, e.g. specific elastic properties, are important attributes to control especially when designing dosage forms that can endure handling and storage. The mechanical properties of the final dosage form can be estimated computationally: The estimation requires the construction of a 3D CAD generated structure, resembling for instance a cross-section of an extrudate (Fig. 2c). Such a structure can subsequently be subjected to a given computational vertical load exerted by a rigid object (reaching 2522 N). Furthermore, by using appropriate values for the Young's modulus (e.g. 3.2 GPa), the density (e.g. 1190 kg/m^2) and the Poisson's ratio (e.g. 0.35) of the mixture, the resulting deformation can be visualized (Fig. 2d). Based on these calculations, the deformation under a given load can be calculated using the geometry, the Young's modulus, the density, and the Poisson's ratio of the object, and the load as input parameters. Shang et al. have previously investigated modeling of tablet breaking using the finite element method.[27]

3.1.3. Simulation of the dissolution properties of the drug product

Dissolution rate of the given drug formulation is another relevant property to investigate. Boetker *et al.* have previously investigated modeling of dissolution within a UV imaging setup.[28] Such calculations of the dissolution of the formulation require the solubility concentration (e.g. 1 mol/m^3) and diffusivity (e.g. $1 \cdot 10^{-9}$ m^2/s) in a given dissolution medium as input parameters, and the concentration change over time can then be solved computationally (Fig. 2e). A computational evaluation of the dissolution rate may be especially useful when designing personalized medicine due to the infinite number of possible designs that may result in different dissolution rates of the given product. Based on these calculations, the dissolution rate of an object in a given media can be calculated using the geometry, the solubility concentration and the diffusivity of the compound in the media as input parameters.

3.2 Experimental support for in silico product design

3.2.1. Rheological analysis

Most pure polymers are shear thinning in nature and their viscosity is highly dependent on temperature. Typically three different regions can be distinguished in their viscosity vs. shear rate curve: zero-shear viscosity η_0 (1st Newtonian plateau), where the viscosity is independent of the shear rate, transition area with the shift from η_0 to shear thinning area, and the power-law area with shear thinning following the power-law function, . Here, shear viscosity (η_s) decreases as a function of shear rate ($\dot{\gamma}$) with a constant slope ($n-1$), and the degree of shear thinning is governed by the power-law coefficient, n.

The results from the SAOS and SS tests for PEO; an absolute value of complex viscosity () and shear viscosity (η_s) vs. angular frequency (ω) and shear rate ($\dot{\gamma}$), respectively, are shown in Fig. 3a. The results indicate that the empirical Cox-Merz rule[29]:, when $\dot{\gamma} = \omega$, is valid for PEO. The fitted Carreau-Yasuda model (solid line in Fig. 3a) had R^2 values of 0.9991, 0.9994, and 0.9994 for the datasets of 100, 130, and 160 °C, respectively.

With a high content of undissolved API, rheological behavior of the mixture is radically different from the pure polymer: Concentrated solid dispersions often show yield stress below which no flow occurs, and the zero-shear viscosity plateau at low shear rates vanishes. In such a case, the Carreau-Yasuda model cannot provide a satisfactory fit, but various models for viscoplastic materials can describe the behavior more accurately.[30-32] The effect of the API content was demonstrated for paracetamol (PRC) – PEO system. The SAOS measurements done at 130 °C for the hot-melt extruded mixtures show plasticization with PRC content up to 50 %, and an increase in viscosity level with yield stress at low frequency for the mixture containing 70 % PRC (Fig. 3b). The results presented here demonstrate the importance of the rheological characterization for accurate predictions and realistic simulations of processes involving flow of molten API-polymer systems.

3.2.2. Solid state analysis

One of the critical quality attributes for a hot melt extruded product is the solid state characteristics of the extrudates that may change during processing. Such changes may not only have a major effect on bioavailability, but also a direct impact on the mechanical properties of the extrudates. It was observed that nitrofurantoin monohydrate (NFMH), a typical isolated site hydrate, dehydrates with an onset temperature around 100°C during a thermogravimetric analysis (TGA, theoretical weight loss 7.0 %, experimental weight loss 6.9%, data not shown). However, as shown in Fig. 4, dehydration of NFMH to the nitrofurantoin anhydrate (NFAH) form is observed in the hot melt extruded NF-PEO mixture already at operating temperatures of around 70°C, markedly lower than the dehydration temperature observed during a typical off-line preformulation study performed with TGA. The degree of dehydration was dependent on the recirculation time of the mixture in the hot-melt extruder: A more pronounced dehydration occurred with a 5 min recirculation time, compared to direct extrusion (recirculation time 0 min), observed as reduction in the * labeled monohydrate peak and an increase in the + label anhydrate peak over time (Fig. 4).

3.2.3. Chemical imaging

Experimental investigations of the API distribution in the extrudates were further explored using NIR imaging combined with multivariate data analysis of the extrudates. Such an NIR imaging setup can be employed in a process analytical technology (PAT) setup where all the products prepared are imaged and these images may subsequently be used for real-time release testing of the products. Other options for performing PAT on hot-melt extrusion processes have previously been investigated using Raman probes[33] and NIR probes[34]. Fig. 5 displays the NIR spectra of the starting materials; here it is possible to obtain data on the ratio of NFMH to PEO since the different species exhibit non-overlaying features in their NIR spectra.

The score surface images and loadings of PC1 and PC2 are depicted in Fig. 6b and d, respectively. The first loading of the PCA model (Fig. 6b) explained 71.9% of the variation and could be correlated to the surface texture variation. The second loading (Fig. 6d) explained 22.4% of the variation and had characteristic bands at 1285, 1480 and 1520nm. The appearance of these bands indicates that the variation captured by principal component 2 can be correlated to the pure spectrum of PEO shown in Fig. 5. Therefore, variation captured by the second loading could be related to the variation of PEO content among the extrudates. The score surface image (Fig. 6c) also indicates that extrudate A, which has a higher concentration of PEO, also has higher score values compared to

extrudate C, which contains a lower concentration of PEO. Based on the score surface image it was possible to distinguish among different extrudates as a function of PEO content that, in turn, could be correlated to the API content. High score values are indicated by the dark red, and low score values by dark blue color. The remaining PCs did not include additional information and the data are not shown. The utilization of NIR imaging in combination with multivariate data analysis may thus provide means for establishing a continuous monitoring of the HME process, which is a prerequisite for the production of personalized medicine.

It can be summarized that the materials science simulation is capable of supporting the design of customizable dosage forms intended for personalized medicine. The simulation approach is required to design the possibly infinite amount of different dosage forms, and PAT is needed to control the product quality in the future manufacturing-on-demand based health-care scenario. Fig. 7 displays the schematic outline of the simulation and experimental tools necessary to control and monitor a given manufacturing process. The optimization of API content and spatial location is needed in order to make the product truly personalized where it is given that each product may contain different amounts of API and potentially different APIs as a combination product. On the experimental side, spectroscopic techniques such as NIR and Raman can be used for both qualitative and quantitative assessments of the API:polymer mixtures. During manufacturing, powder flow and process simulations may be carried out in advance to account for new values of the API and excipient ratios that may for instance instigate different powder flow properties. Furthermore monitoring and recording CQA (critical quality attributes) based on chemical imaging PAT tools, such as NIR and Raman, can be used to provide useful documentation of the product for the regulatory authorities. At the final product level, chemical imaging, dissolution and mechanical strength tests are required in order to validate the various simulations.

4. Conclusions

It has been demonstrated that *in silico* based product design principles can be successfully applied to visualize both deformation and stresses on extruded systems as well as to assessing the dissolution rate from the extruded product. Experimental investigations can be used to provide complimentary information on the solid state properties, such as dehydration kinetics of the extruded product, and to establish the means for achieving continuous monitoring and production of the product. In addition, rheological evaluation of molten polymer based products is crucial for determining optimal HME processing conditions. A computational approach combined with experimental investigations conveys several advantages that are indeed required in the pursuit of designing the future manufacturing solutions within the area of personalized medicine. Finally, a PAT approach is a prerequisite for robust quality control of personalized medicines.

5. ACKNOWLEDGEMENTS

The Danish Council for Independent Research (DFF), Technology and Production Sciences (FTP), Project 12-126515/0602-02670B (2013-2017) and the Lundbeck Foundation, project R108-A108760.

5. References

[1] Treffer D, Wahl P, Markl D, et al., *Hot Melt Extrusion as a Continuous Pharmaceutical Manufacturing Process*, in *Melt Extrusion*, M.A. Repka, N. Langley, and J. DiNunzio, Editors. 2013, Springer New York. p. 363-396.

[2] Son D, Lee J, Qiao S, et al., *Multifunctional wearable devices for diagnosis and therapy of movement disorders.* Nat Nanotechnol, 2014. **9**(5): p. 397-404.

[3] Scheffler M and Hirt E, *Wearable devices for telemedicine applications.* Journal of telemedicine and telecare, 2005. **11 Suppl 1**: p. 11-4.

[4] Rantanen J and Khinast J, *The Future of Pharmaceutical Manufacturing Sciences.* J Pharm Sci, 2015.

[5] Selen A, Dickinson P A, Mullertz A, et al., *The Biopharmaceutics Risk Assessment Roadmap for Optimizing Clinical Drug Product Performance.* J Pharm Sci, 2014. **103**(11): p. 3377-3397.

[6] Colombo P, Sonvico F, Colombo G, et al., *Novel Platforms for Oral Drug Delivery.* Pharm Res-Dord, 2009. **26**(3): p. 601-611.

[7] Losi E, Bettini R, Santi P, et al., *Assemblage of novel release modules for the development of adaptable drug delivery systems.* Journal of Controlled Release, 2006. **111**(1-2): p. 212-218.

[8] Repka M A, Shah S, Lu J N, et al., *Melt extrusion: process to product.* Expert Opin Drug Del, 2012. **9**(1): p. 105-125.

[9] Rowe C W, Katstra W E, Palazzolo R D, et al., *Multimechanism oral dosage forms fabricated by three dimensional printing (TM).* J. Control. Release, 2000. **66**(1): p. 11-17.

[10] Zieverink J, *FDA APPROVES THE FIRST 3D PRINTED DRUG PRODUCT. https://aprecia.com/pdf/2015_08_03_Spritam_FDA_Approval_Press_Release.pdf.* 2015.

[11] Janssen H A, *Versuche über Getreidedruck in Silozellen.* Zeitschr. d. Vereines deutscher Ingenieure, 1895. **39**(35): p. 1045-1049.

[12] Ayuga F, Guaita M, and Aguado P, *Static and dynamic silo loads using finite element models.* J Agr Eng Res, 2001. **78**(3): p. 299-308.

[13] Vidal P, Gallego E, Guaita M, et al., *Finite element analysis under different boundary conditions of the filling of cylindrical steel silos having an eccentric hopper.* J Constr Steel Res, 2008. **64**(4): p. 480-492.

[14] Guaita M, Couto A, and Ayuga F, *Numerical simulation of wall pressure during discharge of granular material from cylindrical silos with eccentric hoppers.* Biosyst Eng, 2003. **85**(1): p. 101-109.

[15] Wu Y H and Schmidt L C, *A Boundary Element Method for Prediction of Silo Pressures.* Comput Struct, 1992. **45**(2): p. 315-323.

[16] Ding S, Rotter J M, Ooi J Y, et al., *Development of normal pressure and frictional traction along the walls of a steep conical hopper during filling.* Thin Wall Struct, 2011. **49**(10): p. 1246-1250.

[17] Young C R, Crowley M, Dietzsch C, et al., *Physicochemical properties of film-coated melt-extruded pellets.* J Microencapsul, 2007. **24**(1): p. 57-71.

[18] De Brabander C, Van den Mooter G, Vervaet C, et al., *Characterization of ibuprofen as a nontraditional plasticizer of ethyl cellulose.* J Pharm Sci, 2002. **91**(7): p. 1678-1685.

[19] Liu H, Zhang X, Suwardie H, et al., *Miscibility studies of indomethacin and Eudragit® E PO by thermal, rheological, and spectroscopic analysis.* J Pharm Sci, 2012. **101**(6): p. 2204-2212.

[20] Aitken-Nichol C, Zhang F, and McGinity J, *Hot Melt Extrusion of Acrylic Films.* Pharm Res-Dord, 1996. **13**(5): p. 804-808.

[21] Yang M, Wang P, Suwardie H, et al., *Determination of acetaminophen's solubility in poly(ethylene oxide) by rheological, thermal and microscopic methods.* Int J Pharmaceut, 2011. **403**(1-2): p. 83-89.

[22] Eitzlmayr A, Koscher G, Reynolds G, et al., *Mechanistic modeling of modular co-rotating twin-screw extruders.* Int J Pharmaceut, 2014. **474**(1-2): p. 157-176.
[23] Eitzlmayr A, Koscher G, Reynolds G, et al., *Mechanistic modeling of modular co-rotating twin-screw extruders.* Int J Pharm, 2014. **474**(1-2): p. 157-76.
[24] Eitzlmayr A and Khinast J, *Co-rotating twin-screw extruders: Detailed analysis of conveying elements based on smoothed particle hydrodynamics. Part 1: Hydrodynamics.* Chemical Engineering Science, 2015. **134**: p. 861-879.
[25] Eitzlmayr A, Khinast J, Horl G, et al., *Experimental Characterization and Modeling of Twin-Screw Extruder Elements for Pharmaceutical Hot Melt Extrusion.* AIChE Journal, 2013. **59**(11): p. 4440-4450.
[26] Sogaard S V, Pedersen T, Alleso M, et al., *Evaluation of ring shear testing as a characterization method for powder flow in small-scale powder processing equipment.* Int J Pharm, 2014. **475**(1-2): p. 315-23.
[27] Shang C, Sinka I C, and Pan J, *Modelling of the break force of tablets under diametrical compression.* Int J Pharm, 2013. **445**(1-2): p. 99-107.
[28] Boetker J P, Rantanen J, Rades T, et al., *A New Approach to Dissolution Testing by UV Imaging and Finite Element Simulations.* Pharm Res-Dord, 2013. **30**(5): p. 1328-1337.
[29] Cox W P and Merz E H, *Correlation of Dynamic and Steady Flow Viscosities.* J Polym Sci, 1958. **28**(118): p. 619-622.
[30] Kalyon D M, Lawal A, Yazici R, et al., *Mathematical modeling and experimental studies of twin-screw extrusion of filled polymers.* Polymer Engineering and Science, 1999. **39**(6): p. 1139-1151.
[31] Papanastasiou T C, *Flows of Materials with Yield.* Journal of Rheology, 1987. **31**(5): p. 385-404.
[32] Mitsoulis E, *Flows of viscoplastic materials: Models and Computations.* Rheology Reviews, 2007: p. 135-178.
[33] Saerens L, Dierickx L, Lenain B, et al., *Raman spectroscopy for the in-line polymer-drug quantification and solid state characterization during a pharmaceutical hot-melt extrusion process.* Eur J Pharm Biopharm, 2011. **77**(1): p. 158-163.
[34] Wahl P R, Treffer D, Mohr S, et al., *Inline monitoring and a PAT strategy for pharmaceutical hot-melt extrusion.* Int J Pharmaceut, 2013. **455**(1-2): p. 159-168.

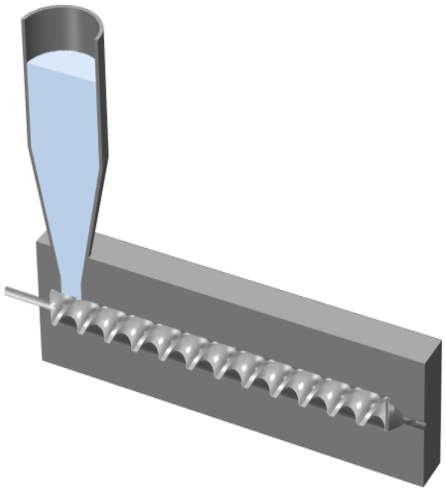

Fig. 1. Schematic representation of a hot-melt extruder with hopper and barrel in dark grey. Powder in light blue and screw in light grey.

a) b)

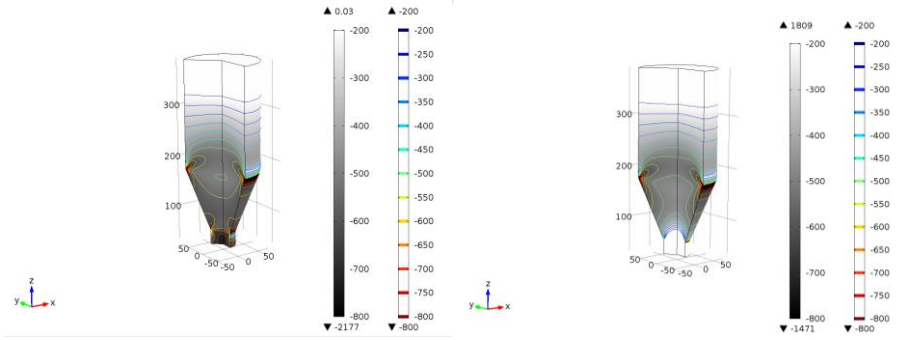

c) d)

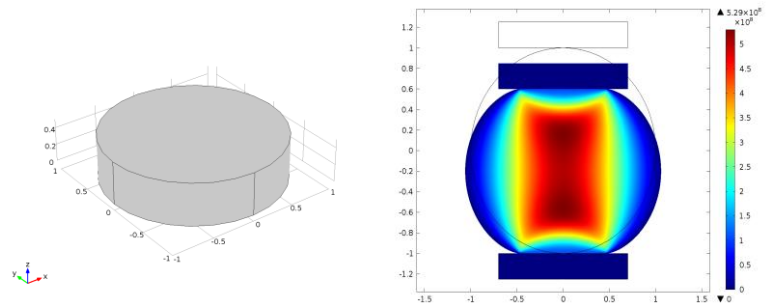

e)

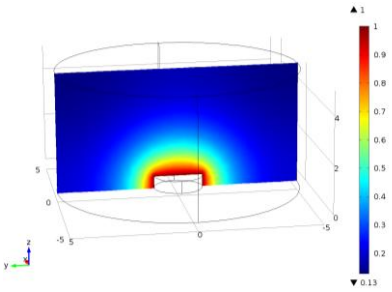

Fig. 2. *In silico* process and product design of a hot melt extruded dosage form. (a) Rotated 2D axisymmetric representations of stress tensor in the downward direction prior to feeding of an extruder (units are given in Pa). (b) Rotated 2D axisymmetric representations of stress tensor in the downward direction during feeding of an extruder (units are given in Pa). (c) Design of a CAD geometry representing a cross-section of an extrudate with 10 mm Ø and a height of 2 mm. (d) 2D Simulation of a deformation of the sliced extruded strand geometry under a vertical load (units are given in N/m^2 and represent the von Mises stress). (e) Simulation of the dissolution of the sliced extrudate strand geometry displaying the concentration gradients from the tablet surface (units are given in mol/m^3).

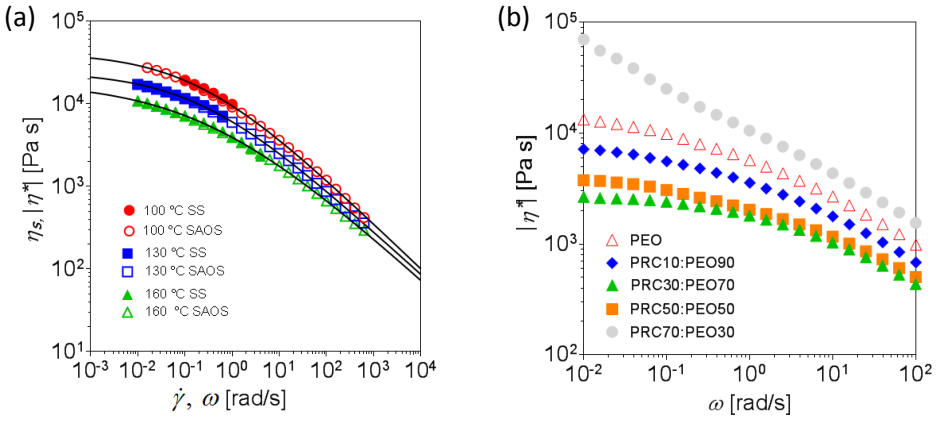

Fig. 3. (a) Viscosity of polyethylene oxide measured at 100, 130, and 160 °C in oscillatory (SAOS, open symbols) and steady-state rotational shear (SS, filled symbols). The continuous line is represents the Carreau-Yasuda model fitted to both SS and SAOS data. (b) Complex viscosity (T= 130 °C) of PEO and extruded PRC:PEO mixtures at PRC content of 10, 30, 50, and 70 %, the last one showing yield stress (no plateauing towards zero-shear viscosity).

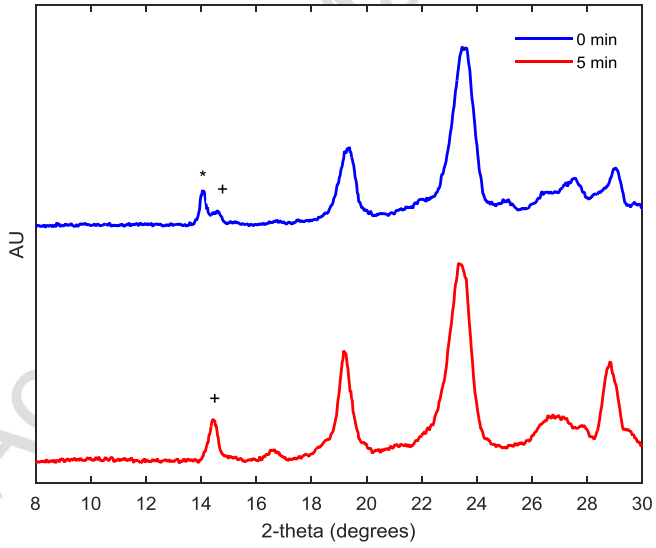

Fig. 4. X-ray powder diffractograms displaying anhydrate and monohydrate forms of nitrofurantoin in the extruded products (with starting material 30:70 NFMH:PEO) with recirculation times of 0 and 5 minutes (* and + are characteristic diffractions of monohydrate and anhydrate, respectively).

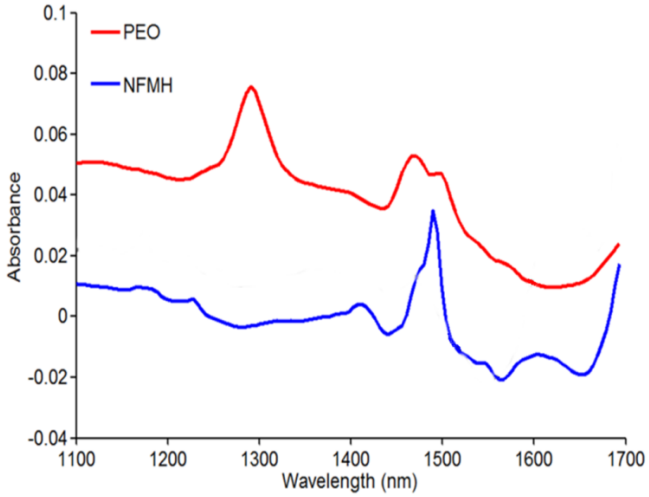

Fig. 5. NIR spectra of starting materials, polymer PEO and the active compound (nitrofurantoin monohydrate, NFMH).

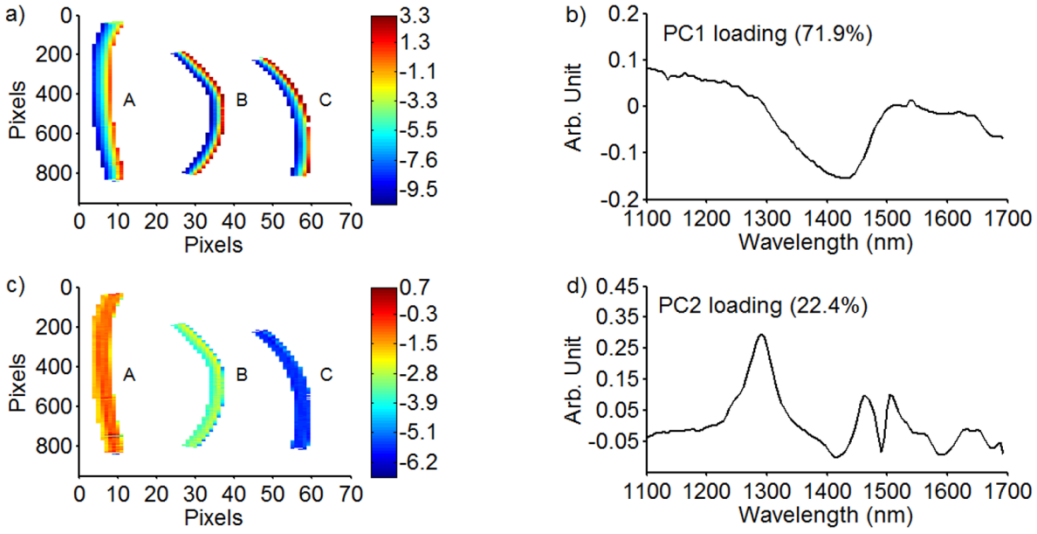

Fig. 6. a and b, represent the score surface image and loading of the first principal component where, c and d, represent for the second principal component. Extrudates, A, B and C, have varying ratios of NFMH:PEO, 30:70, 50:50 and 70:30, respectively.

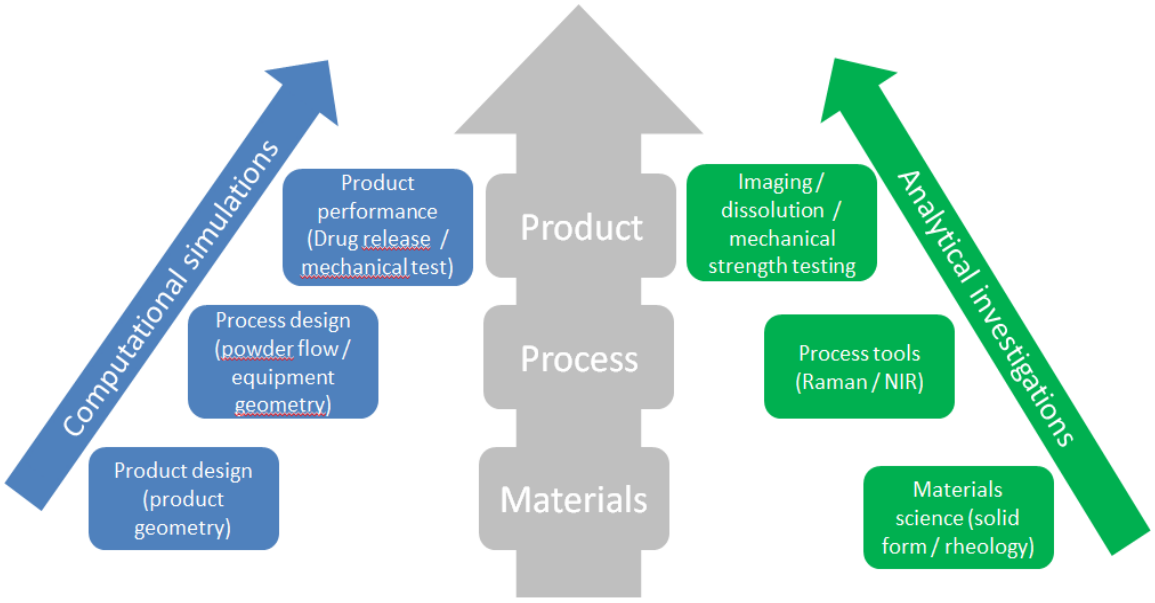

Fig. 7. Schematic presentation of the simulation tools (blue) and analytical tools (green) needed for monitoring and controlling a given production manufacturing (grey).